01 May 2016

Direct Printing of Microstructures by Femtosecond Laser Excitation of Nanocrystals in Solution

W. Shou

Heng Pan

Missouri University of Science and Technology, hp5c7@mst.edu

Direct printing of microstructures by femtosecond laser excitation of nanocrystals in solution

Wan Shou, and Heng Pan

Citation: Appl. Phys. Lett. **108**, 214101 (2016); doi: 10.1063/1.4952615
View online: https://doi.org/10.1063/1.4952615
View Table of Contents: http://aip.scitation.org/toc/apl/108/21
Published by the American Institute of Physics

Direct printing of microstructures by femtosecond laser excitation of nanocrystals in solution

Wan Shou and Heng Pan[a)]
Department of Mechanical and Aerospace Engineering, Missouri University of Science and Technology, Rolla, Missouri 65401, USA

(Received 13 March 2016; accepted 11 May 2016; published online 24 May 2016)

We report direct printing of micro/sub-micron structures by femtosecond laser excitation of semiconductor nanocrystals (NCs) in solution. Laser excitation with moderate intensity (10^{11}–10^{12} W/cm^2) induces 2D and 3D deposition of CdTe nanocrystals in aqueous solution, which can be applied for direct printing of microstructures. It is believed that laser irradiation induces charge formation on nanocrystals leading to deposition. Furthermore, it is demonstrated that the charged nanocrystals can respond to external electrical bias, enabling a printing approach based on selective laser induced electrophoretic deposition. Finally, energy dispersive X-ray analysis of deposited structures shows oxidation occurs and deposited structure mainly consists of Cd_xO. *Published by AIP Publishing.*
[http://dx.doi.org/10.1063/1.4952615]

Generally, direct writing using single or multiple energized beams (e.g., laser, ion, or electron beams) provides high feature resolution (<1 μm) compared with other solution-based printing methods (e.g., inkjet printing). There have been extensive research on micro/nanoadditive manufacturing methods employing laser (or optical) and ion/electron beams, including micro-stereolithography,[1] two-photon polymerization,[2] microselective laser sintering,[3] laser (including focused ion beam) Chemical Vapor Deposition (CVD),[4,5] MAPLE,[6,7] and laser induced precipitation and reduction.[8–12] Many of these processes utilize specially designed photosensitive materials consisting of additives and effective components. Due to the presence of additive (such as polymer and binders), the effective components are relatively low resulting in a high threshold for device operation. Laser CVD can effectively remove polymer components at the cost of expensive vacuum equipment. Laser induced reduction has limited control over the processing condition, which strongly influences the final structures.

In order to direct print functional devices at low cost, there has been extensive research on laser processing of pre-synthesized nanomaterials for non-polymer functional device manufacturing. Pre-synthesized nanocrystals can have better control in the stoichiometry and crystallinity. In addition, *pre-synthesis* process enjoys the flexibility in material choice since a variety of materials can be synthesized. Laser induced forward transfer has been used to print pre-synthesized nano-ink to form 2D conductive patterns.[13] Laser sintering and ablation of functional nanomaterials has led to unprecedented advantages for microadditive manufacturing of electronics.[14,15] Recently, a tightly focused fs laser has been used to assemble CdTe quantum dots and form nanoscale 2D patterns (down to 170 nm).[16] Functional devices such as chemical sensors[16] and conductors[17] have been demonstrated. The researchers suggested the assembly mechanism is due to laser trapping force.[16] A majority of the demonstrated laser assembly of nanocrystals are 2D processes. Adopting a process similar to femtosecond laser two-photon lithography, 3D assembly of functional graphene oxide has been recently demonstrated.[18]

Femtosecond laser assembly and deposition of nanomaterials can be a feasible 3D micro/nanoadditive manufacturing approach, although mechanisms leading to assembly and deposition have not been fully understood. It is suggested that laser trapping force could be one mechanism leading to assembly.[16] In this paper, we propose a mechanism for 2D and 3D deposition of nanocrystals by laser excitation with moderate peak intensities (10^{11}–10^{12} W/cm^2). The method does not rely on laser trapping. It is postulated that laser induced charging is responsible for the deposition. In addition, the scheme paves the way for laser selective electrophoretic deposition as a micro/nanoscale additive manufacturing approach.

The experimental setup is shown in Fig. 1(a). A femtosecond laser (Calmar Cazadero) with 1030 nm wavelength,

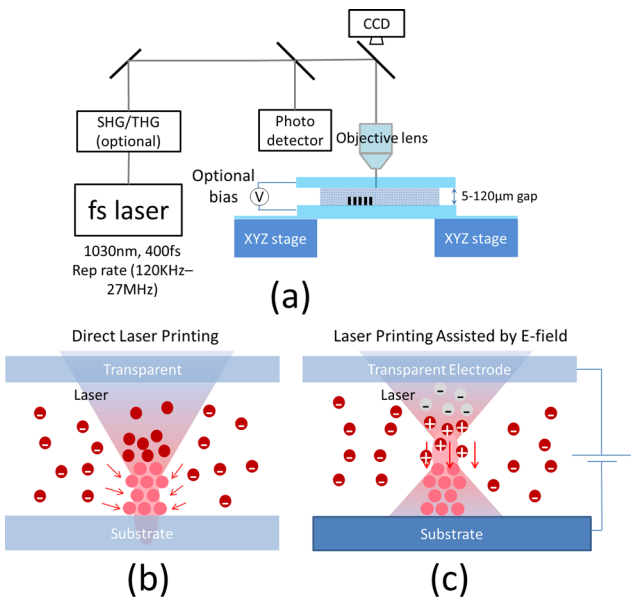

FIG. 1. (a) Experimental setup for femtosecond laser nanomaterial printing. (b) Printing by using laser only. (c) Printing by laser and external bias.

[a)]Author to whom correspondence should be addressed. Electronic mail: hp5c7@mst.edu

400 fs pulse width, and adjustable repetition rates (120 kHz–27 MHz) was employed. To minimize the laser trapping effect, a low NA = 0.43 lens (20×, 2.6 μm spot size) was employed. CdTe quantum dots functionalized by carboxylic acid (Sigma) was dispersed in aqueous solution (3–4 nm size, 1 wt. %, pH = 7). The zeta potential of the as-prepared CdTe QDs solution was measured around −41 mV (negative charges). An optional electrical bias can be applied using transparent electrodes across the gap to assist directional deposition.

Femtosecond laser was focused near the bottom substrate, as shown in Fig. 1(a), to determine the threshold laser intensity to induce deposition. With laser power at 60 mW and repetition rate at 2.7 MHz (peak intensity $\sim 9.59 \times 10^{11}$ W/cm^2), deposition can be observed after several seconds of irradiation. At this threshold intensity level, depositions were found to scatter within the laser irradiated area (Fig. 2(a-i)). The scattered deposition covering a large area within the laser irradiated area (instead of gathering at the center of the laser focal spot) indicates the deposition is unlikely due to optical trapping. We can estimate the gradient force needed to realize optical trapping. To trap nanoparticles (NPs), the optical gradient force should be $>10^{-14}$ N (Refs. 16, 19, and 20) to overcome the diffusion driven by thermal energy k_BT. To irreversibly assemble NPs after trapping, the electrostatic (ES) repulsion needs to be overcome. The primary ES energy barrier is a few times of k_BT depending on measured Zeta potential.[21] This means the optical force should at least a few times of 10^{-14} N to overcome both the ES repulsion between NPs and thermal diffusion. This is in agreement with literatures reported laser intensities for optical trapping of CdTe quantum dots.[21] Using measured polarizability,[19] reported averaged laser intensities are converted to gradient forces. It can be seen that the averaged laser intensity should be >10 MW/cm^2 to generate gradient force $>2 \times 10^{-14}$ N, for both fs and CW laser near 1030 nm. The average laser intensity is 0.5–1.5 MW/cm^2 in this work, which only yields gradient force from 1.5×10^{-16} to 4.5×10^{-16} N. Therefore, it is concluded that the deposition observed in this work is unlikely due to optical trapping force. As the laser intensity increases, the deposition becomes clear. The deposition rate is clearly higher at the laser spot center, suggesting that the deposition is laser intensity dependent. Furthermore, it is found that the threshold intensity depends on repetition rates, as plotted in Fig. 2(b). With lower repetition rate (longer time between pulses), higher peak laser intensity will be required to induce deposition. The effects of laser powers (above deposition threshold) and repetition rates on deposition size are summarized in Fig. 2(c). Finally, the capability of this process in fabricating lines and dots arrays is shown in Fig. 2(d).

It appears that laser irradiation generates "activated nanocrystals" within the laser focal spot that tend to be deposited or aggregated. The substrate was then moved to various z positions within the depth of focus to study the deposition pattern. With laser focused at 6 μm below the substrate, the deposition appears to be smaller than the deposition at focal plane (z = 0). The concentration of "activated nanocrystals" is expected to correlate with laser intensity within the laser focal volume. With the laser located 6 μm below the substrate, only the center area receives laser intensity above the threshold level, which leads to a smaller deposition. The laser is moved above the substrate (z = 9 μm), slightly smaller spot can be observed as expected. Interestingly, in this case instead of forming a flat deposition, the deposition appears to be extended in z direction (3D structure), as shown in Fig. 3(a-iv). The "activated nanocrystals," which are generated within the entire elongated volume of the laser focal spot above the substrate, will interact with each other while they diffuse towards the substrate. Once a deposition is formed on the substrate, more in-coming "activated nanocrystals" formed above the substrate will continue to be deposited and extend the structure in the z direction. Utilizing this spatial distribution of "activated nanocrystals," a 3D structure was formed by vertically moving the laser. Laser was initially focused at z = 7 μm above the substrate and slowly moved to z = 16 μm within 30 s. A pillar structure was formed with the height around 3–4 μm by the laser guided deposition (Fig. 3(b)).

It is postulated that laser irradiation induce charges on nanocrystals, which alters the electrostatic potential between NCs. To verify the charge formation, the top and bottom glass substrates were replaced with transparent conductive electrodes such that electrical bias can be applied. The electrode gap was maintained at $\sim$100 μm, and laser spot was located z = 40 μm above the substrate (far enough from the substrate to avoid any direct laser induced deposition). As can be seen in Fig. 4(a-i), with laser power at 30 mW and voltage at 2.9 V,

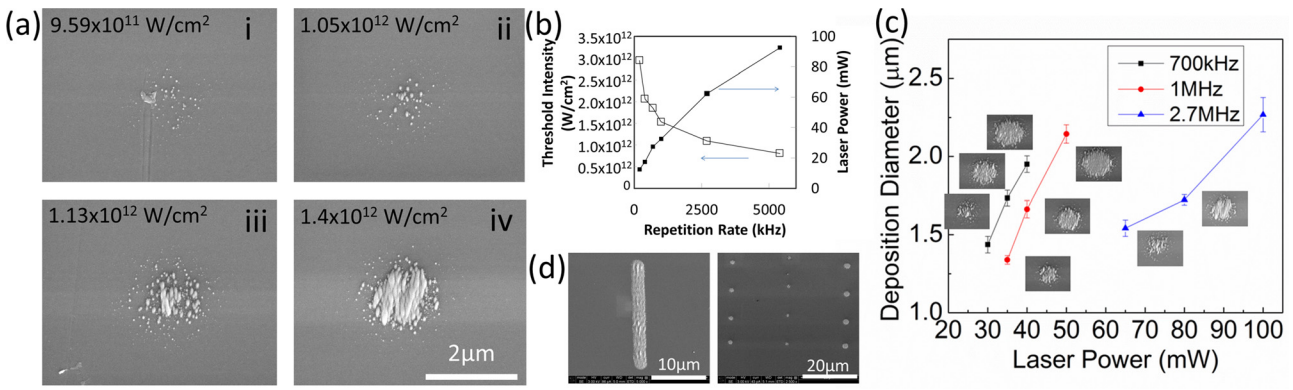

FIG. 2. (a) Laser induced deposition at various level of laser peak intensity. (b) Laser intensity threshold to induce deposition at various repetition rate. (c) Measured deposition diameters after 10 s laser irradiation from SEM images under various laser powers and repetition rates. (d) Fabricated two-dimensional patterns including lines and dots array.

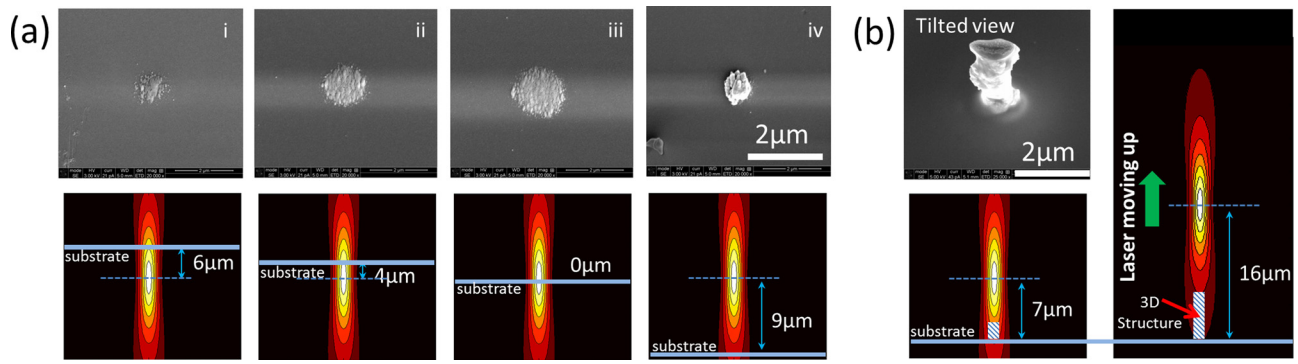

FIG. 3. (a) Deposition patterns with substrate located above (i, ii), at (iii), and below (iv) focal plane. (b) 3D structure fabricated by moving laser vertically from z = 7 μm to z = 16 μm.

no deposition was observed. By slightly increasing the voltage to 3.0 V, noticeable depositions were immediately observed directly below the laser spot (Fig. 4(a-ii)). The zeta potential of un-processed CdTe nanocrystal was measured to be around −41 mV (negative charges). The fact that the NCs were attracted to the negatively charged cathode after laser excitation suggests the charge in the particle might have been reversed.

E-field assisted laser induced deposition under various laser intensities and bias voltages are summarized in the supplementary material[21] (Fig. S2 and Fig. 4(b)). With laser power maintained at 30 mW, increasing voltage from 2.9 to 3.1 V substantially increases the amount of deposition. It is also noted that the amount of deposition increases with the increase in deposition time from 10 to 20 s. However, a further increase in deposition time from 20 to 30 s does not necessarily lead to more deposition for the cases with low bias voltages (2.9 and 3.0 V), suggesting that the laser generated "activated nanocrystals" might have been depleted. In this medium laser power and low voltage range, the deposition exhibits a disk shaped morphology.[21] Increasing laser power from 30 to 35 mW leads to the increase in the deposition amount and truncated cone shaped deposition appears. High laser power generates more "activated nanocrystals" that can be electrical biased towards the bottom substrate. However, an excessive amount of "activated nanocrystals" could result in uncontrollable and non-uniform deposition. In order to improve the deposition quality, lower laser power and high bias are preferred. This can be observed by 25 mW and 3.5 V deposition (low laser power and high bias), and more regular pattern with rounded shapes can be printed, which can be identified as a hemisphere mode. The hemisphere mode also exhibits more controllable deposition manifested by a steady increase in the deposition volume with deposition time (Fig. 4(b)). The estimated deposition volume with respect to time under three modes of deposition are summarized in Fig. 4(b) (with details on volume calculation in the supplementary material[21]). A low laser intensity with higher voltage will avoid excessive "activated particles" and enhance directionality of these particles such that deposition with better quality and smaller features could be realized.

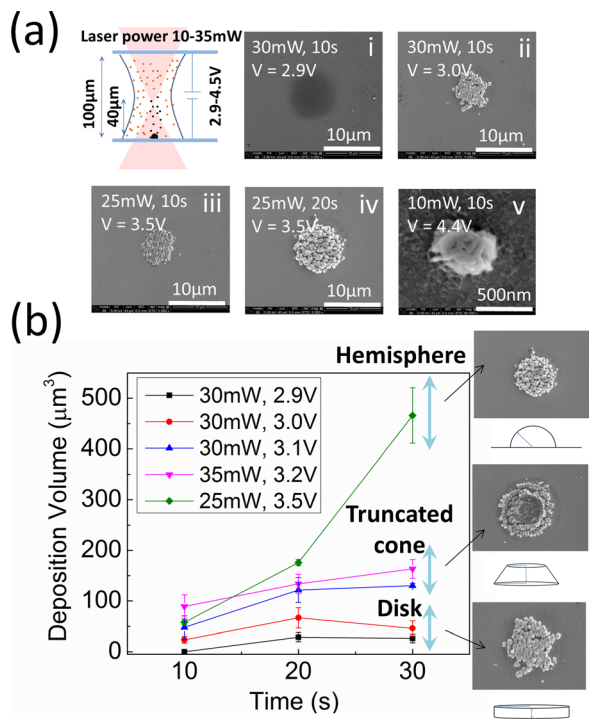

FIG. 4. Laser printing assisted by applied voltage. (a) SEM images of deposition under various laser powers and voltages. (i) Laser power 30 mW, bias 2.9 V, deposition time 10 s; (ii) Laser power 30 mW, bias 3.0 V, deposition time 10 s; (iii) Laser power 25 mW, bias 3.5 V, deposition time 10 s; (iv) Laser power 25 mW, bias 3.5 V, deposition time 20 s; (v) Laser power 10 mW, bias 4.4 V, deposition time 10 s. (b) Quantitative measurement of deposition volume under various laser powers and voltages.

To test this, laser power was further reduced to 10 mW (peak intensity is 6.5×10^{11} W/cm^2) and the bias increased to 4.4 V. A sub-micron feature with a diameter ~500 nm, which is substantially smaller than the laser spot (2.6 μm), can be deposited, as shown in Fig. 4(a-v). The sub-micron feature could be formed due to collisions of the "activated nanocrystals" before reaching the substrate, or after reaching the substrate. Considering the distance the nanocrystals need to travel from the laser focal spot to the substrate ($L \sim 40$ μm) and assuming q = +4, the travel time under electrophoretic force can be estimated as $L/V_e \sim 30$ ms, where $V_e = Eq/(4\pi R\eta)$ is the velocity of the charged particle under E-field, E is the electrical field, η is the viscosity, and R is the NP radius. It is believed that the charge life-time on NPs should be at similar scale (>10 ms) or longer. Using the Stokes-Einstein relation, $D = k_B T/(f\pi\eta R)$,[22] where k_B is Boltzmann constant, T is the temperature, and f is a constant, the calculated diffusivity D of the NP is $\sim 1.6 \times 10^{-10}$ m^2/s. The lateral diffusion length $\sqrt{Dt}$ would suggest $(D \times 30\,\text{ms})^{0.5} \sim 2$ μm,

4 times larger than 500 nm. Therefore, it is believed that the particles collide and form the sub-micron structure of ~500 nm before reaching the substrate. Assuming Brownian motion, the average collision time between collisions is $\eta/(Nk_BT) \sim 1$–$10\ \mu s$,[23] where N ($7 \times 10^{22}\ m^{-3}$) is the NP concentration, which is much shorter than the travel time (~30 ms). Thus, it is reasonable to believe the nanocrystals have sufficiently collided and form sub-micron aggregate before reaching the substrate.

We furthermore measured the induced current under bias in order to estimated laser induced charge on each particle. It was determined that the current increases by ~15 nA when 30 mW laser irradiation turns on (voltage is ~3.5 V). The current between two electrodes will read $I = 2N\mu ZVA/d$, where μ is the electrophoretic mobility, N is the NP concentration, Z is the NP charge, V is the applied voltage, A is the electrode area, and d is the gap distance.[24] The μ is related to zeta potential using theory of electrophoresis, and zeta potential is realted to charges Z from electrostatics. This way, by measuring current I, laser induced eletrophoretic mobility μ (or charges Z) can be estimated. Using the measured current and deposited area $A \sim 100\ \mu m^2$, the electrophoretic mobility is estimated to be $+6.6 \times 10^{-8}\ m^2\ V^{-1}\ S^{-1}$, which corresponds to ~7 charges per particle.

Femtosecond laser could induce charges on irradiated semiconductor nanocrystals. There could be two paths to form charges. First, laser can induce excitation of electrons into conduction band where excited state can react with species in water to form charge species. Assuming two-photon absorption coefficient is 210 for CdTe quantum dots,[25] 30 mW@700 kHz repetition rate, and quantum yield 10^{-4} (percentage of excited electron interact with species), one would estimate $\sim 2 \times 10^3$ excited electrons are formed in conduction band that can react with species per particle per second. This level of excited electron is sufficient for surface reactions to generate charged species (photoelectrophoresis effects). Boxall reported photoelectrophoresis in TiO_2 nanoparticles. Using the experiment conditions by Boxall:[26] $\sim 0.1\ W/cm^2$ for light intensity, $10^{-12}\ cm^2$ for NP absorption cross section, and 10^{-4} for quantum yield. It can be estimated that around 50 charges are formed per second on each particle. The estimated number of excited electrons in this work is higher than this level; therefore, photoelectrophoresis could be expected. Secondly, the electron could be emitted. Before the emitted electrons recombined, the nanocrystals will be temporally charged. We estimated the electron temperature under moderate laser irradiation and ionization rate considering thermal emission and thermos-assisted photoemission.[27] With 30 mW@700 kHz ($1.95 \times 10^{12}\ W/cm^2$) laser power, two-photon absorption coefficient 210, CdTe NP can emit several electrons per pulse (Te ~ 6000 K). It suggests the possibility of observing positive charges due to electron ejection. The electrons once ejected can form solvated (hydrated) electron.[28] The solvated electrons react with solvent, such as H_2O, to form intermediate species (OH^-). It will take μs to ms before OH^- recombines.[29] Before OH^- recombination, NP is charged and can response to the electric field.

It should be pointed out that the process described above can occur without significantly increasing the solution temperature. This is possible by using (1) fs laser with moderate repetition rates (to achieve high peak power for non-thermal excitations while maintaining lower thermal accumulation) and (2) ultra-fine nanocrystals (to increase thermal dissipation). We have estimated, using the two-photon absorption cross section of nanocrystals and 1 wt. % concentration, the steady state temperature rises are <15 K with averaged laser power <40 mW. Meanwhile, thermal analysis based on single pulse heating shows lattice temperature of nanocrystals can increase by ~100–200 K during the period of single pulse. However, the thermal relaxation time of the nanocrystals in solvent is 14.5 ps, which is shorter than the vaporization time 16 ps (determined by Kapitza resistance);[30] therefore, no nano-bubbles can be formed. In addition, the electron emission density is well below the critical density to generate plasma in solvent.[31]

Energy dispersive X-ray (EDX) compositional profiling was performed on the deposited structure (supplementary material,[21] Fig. S3). The results show main contents are Cd (63 wt. %) and O (31 wt. %) with negligible amount of Te (6 wt. %). The oxygen curve shows obvious peaks and valleys as cadmium does, while tellurium only shows weak and wide peaks in the corresponding locations. These results indicate the deposited materials are oxidized cadmium (Cd_xO) with limited amount of CdTe. It is believed that CdTe is not stable under excitation state and it can be oxidized by aqueous environment.[32] To reduce the oxidation effect, the experiment will be performed in non-aqueous solution and reported in future.

We have reported microstructure printing by femtosecond laser induced charging of nanocrystals. The laser induced printing process can be assisted with electrical bias. The smallest feature fabricated is ~500 nm, substantially lower than the diffraction-limited laser spot size (~2.6 μm). Detailed analysis of deposition mechanisms implies the semiconductor nanocrystals are charged by femtosecond laser irradiation with moderate intensities (10^{11}–$10^{12}\ W/cm^2$). The life time of the induced charges can be longer than tens of milliseconds, which is sufficient to complete the electrophoretic process between two parallel electrodes separated by ~100 μm. This work potentially enables a 2D/3D functional device printing approach with sub-diffraction-limited feature resolutions.

This work was supported financially by Interdisciplinary Intercampus Funding Program (IDIC) of University of Missouri System, University of Missouri Research Board (UMRB), and seed funds from Intelligent System Center (ISC) and Material Research Center (MRC) at Missouri University of Science and Technology. This work was also partially supported by ORAU Ralph E. Powe Junior Faculty Enhancement Award. Their supports are greatly appreciated.

[1]K. Ikuta and K. Hirowatari, in *Proceedings of the IEEE Workshop on Microelectromechanical Systems, MEMS'93* (1993), p. 42.
[2]S. Maruo and S. Kawata, IEEE ASME J. Microelectromech. Syst. **7**, 411 (1998).
[3]M. Vaezi, H. Seitz, and S. Yang, Int. J. Adv. Manuf. Technol. **67**, 1721 (2013).
[4]I. Gibson, D. W. Rosen, and B. Stucker, *Additive Manufacturing Technologies* (Springer, New York, 2010).
[5]D. J. Nagel, *Direct Write Technologies for Rapid Prototyping Applications* (Academic, New York, 2002), p. 557.

[6]A. Pique, C. B. Arnold, R. C. Wartena, B. Pratap, B. Shashishekar, K. E. Swider-Lyons, D. W. Weir, and R. A. Kant, RIKEN Rev. **50**, 57 (2003).
[7]R. Wartena, A. E. Curtright, C. G. Arnold, A. Pique, and K. E. Swider-Lyons, J. Power Sources **126**, 193 (2004).
[8]T. Tanaka, A. Ishikawa, and S. Kawata, Appl. Phys. Lett. **88**, 081107 (2006).
[9]S. Passinger, M. S. M. Saifullah, C. Reinhardt, K. R. V. Subramanian, B. N. Chichkov, and M. E. Welland, Adv. Mater. **19**, 1218 (2007).
[10]W. Lu, Y. Zhang, M. Zheng, Y. Jia, J. Liu, X. Dong, Z. Zhao, C. Li, Y. Xia, T. Ye, and X. Duan, Opt. Mater. Express **3**, 1660 (2013).
[11]T. DeJournett and J. B. Spicer, Phys. Chem. Chem. Phys. **15**, 19753 (2013).
[12]S. Kang, K. Vora, and E. Mazur, Nanotechnology **26**, 121001 (2015).
[13]C. Boutopoulos, I. Kalpyris, E. Serpetzoglou, and I. Zergioti, Microfluid. Nanofluid. **16**, 493 (2014).
[14]S. H. Ko, H. Pan, C. P. Grigoropoulos, C. K. Luscombe, and J. M. J. Frechet, Nanotechnoogy **18**(34), 345202 (2007).
[15]H. Pan, S. H. Ko, and C. P. Grigoropoulos, Appl. Phys. A **90**, 247 (2008); J. Heat Transfer **130**, 092404 (2008); H. Pan, S. H. Ko, N. Misra, and C. P. Grigoropoulos, Appl. Phys. Lett. **94**, 071117 (2009); H. Pan, D. J. Hwang, S. H. Ko, T. A. Clem, J. M. J. Frechet, D. Bauerle, and C. P. Grigoropoulos, Small **6**, 1812 (2010); H. Pan, S. H. Ko, and C. P. Grigoropoulos, J. Appl. Phys. **115**, 104307 (2014).
[16]B. Xu, Y. Zhang, R. Zhang, L. Wang, X. Xiao, H. Xia, Q. Chen, and H. Sun, J. Mater. Chem. C **1**, 4699 (2013).
[17]H. Wang, S. Liu, Y. Zhang, J. Wang, L. Wang, H. Xia, Q. Chen, H. Ding, and H. Sun, Sci. Technol. Adv. Mater. **16**, 024805 (2015).
[18]B. Senyuk, N. Behabtu, A. Martinez, T. Lee, D. E. Tsentalovich, G. Ceriotti, J. M. Tour, M. Pasquali, and I. I. Smalyukh, Nat. Commun. **6**, 7157 (2015).
[19]L. Jauffred, A. C. Richardson, and L. B. Oddershede, Nano Lett. **8**(10), 3376 (2008); **10**, 1927 (2010); L. Jauffred, A. Kyrsting, E. C. Arnspang, S. N. S. Reihani, and L. B. Oddershede, Nanoscale **6**, 6997 (2014).
[20]W. Y. Chiang, T. Okuhata, A. Usman, N. Tamai, and H. Masuhara, J. Phys. Chem. B **118**, 14010 (2014).
[21]See supplementary material at http://dx.doi.org/10.1063/1.4952615 for laser trapping force estimation, deposition morphology and EDX characterizations.
[22]E. A. Mun, C. Hannell, S. E. Rogers, P. Hole, A. C. Williams, and V. V. Khutoryanskiy, Langmuir **30**, 308 (2014).
[23]R. M. Ziff, E. D. McGrady, and P. Meakin, J. Chem. Phys. **82**, 5269 (1985).
[24]M. Cirillo, F. Strubbe, K. Neyts, and Z. Hens, ACS Nano **5**, 1345 (2011).
[25]L. Pan, N. Tamai, K. Kamada, and S. Deki, Appl. Phys. Lett. **91**, 051902 (2007).
[26]C. Boxall and G. H. Kelsall, J. Chem. Soc., Faraday Trans. **87**, 3537 (1991); J. Electroanal. Chem. **328**, 75 (1992).
[27]W. Wendelen, B. Y. Mueller, D. Autrique, B. Rethfeld, and A. Bogaerts, J. Appl. Phys. **111**, 113110 (2012).
[28]M. Haase, H. Weller, and A. Henglein, J. Phys. Chem. **92**, 4706 (1988).
[29]D. N. Nikogosyan, A. A. Oraevsky, and V. I. Rupasov, Chem. Phys. **77**, 131 (1983).
[30]J. Lombard, T. Biben, and S. Merabia, Phys. Rev. Lett. **112**, 105701 (2014).
[31]E. Boulais, R. Lachaine, and M. Meunier, Nano Lett. **12**(9), 4763 (2012).
[32]J. Ma, J. Chen, Y. Zhang, P. Wang, J. Guo, W. Yang, and C. Wang, J. Phys. Chem. B **111**, 12012 (2007).